Liquid Crystals
Publication details, including instructions for authors and subscription information:
http://www.informaworld.com/smpp/title~content=t713926090

Possible transition from rod-like to disc-like behaviour in *ortho*-metallated imine complexes of palladium(II): crystal and molecular structure of three palladium complexes

Laurent Omnès[a]; Viorel Cîrcu[a]; Peter T. Hutchins[a]; Simon J. Coles[b]; Peter N. Horton[b]; Michael B. Hursthouse[b]; Duncan W. Bruce[ac]
[a] Department of Chemistry, University of Exeter, Exeter EX4 4QD, UK [b] EPSRC Crystallographic Service, Department of Chemistry, University of Southampton, Highfield, Southampton SO17 1BJ, UK [c] Present address: Department of Chemistry, University of York, Heslington, York YO10 5DD

To cite this Article Omnès, Laurent , Cîrcu, Viorel , Hutchins, Peter T. , Coles, Simon J. , Horton, Peter N. , Hursthouse, Michael B. and Bruce, Duncan W.(2005) 'Possible transition from rod-like to disc-like behaviour in *ortho*-metallated imine complexes of palladium(II): crystal and molecular structure of three palladium complexes', Liquid Crystals, 32: 11, 1437 — 1447
To link to this Article: DOI: 10.1080/02678290500160753
URL: http://dx.doi.org/10.1080/02678290500160753

Liquid Crystals, Vol. 32, No. 11–12, November–December 2005, 1437–1447

Possible transition from rod-like to disc-like behaviour in *ortho*-metallated imine complexes of palladium(II): crystal and molecular structure of three palladium complexes

LAURENT OMNÈS†, VIOREL CÎRCU†, PETER T. HUTCHINS†, SIMON J. COLES‡, PETER N. HORTON‡, MICHAEL B. HURSTHOUSE‡ and DUNCAN W. BRUCE*†

†Department of Chemistry, University of Exeter, Stocker Road, Exeter EX4 4QD, UK
‡EPSRC Crystallographic Service, Department of Chemistry, University of Southampton, Highfield, Southampton SO17 1BJ, UK

(*Received 28 January 2005; accepted 24 March 2005*)

Two series of *ortho*-metallated palladium imine complexes are reported that contain a coordinated β-diketonate group. In one group the chain length of the imine is varied while the β-diketone is unchanged; in the other the imine chains are both fixed as methoxy and the structure of the β-diketonate is varied. The mesomorphism of these new complexes is reported and discussed in relation to the search for materials showing a biaxial nematic phase.

1. Introduction

The biaxial nematic phase (N_B) was predicted by Freiser in 1970 and has been a topic of intense interest ever since. The phase was demonstrated experimentally by Yu and Saupe [1] in a ternary lyotropic system in 1980 and has been found subsequently in other lyotropic systems [2], but its existence in thermotropic systems has been more controversial. Work on side chain liquid crystal polymers by Finkelmann [3] and by Saalwächter [4] provided examples that were identified by optical and ^{2}H NMR methods, respectively, the latter giving a biaxial order parameter of *c*. 0.15. More recently, reports have appeared [5, 6] of a biaxial nematic phase in oxadiazole mesogens, where NMR methods have revealed a biaxial order parameter of *c*. 0.1. An account of other design approaches and of the results of characterization may be found in four overview articles where experimental approaches to theoretical/computational ideas are also discussed [7–10]. Methods of characterization are considered in a separate overview [11].

This last matter is crucially important and has, in several cases, been the origin of debate and controversy in assigning a phase as N_B. As discussed in [11], there are optical methods for identifying a N_B phase but these are not straightforward and other techniques are potentially more amenable. ^{2}H NMR spectroscopy can provide an unequivocal identification of a N_B phase and has been used in some cases to show that a putative N_B phase is in fact N_U [8]. However, access to the specialist experiments required is not widely available, and there is the additional requirement that candidate compounds need ideally to be deuteriated regiospecifically. However, perhaps a more straightforward method for at least identifying *candidate* materials for more detailed study is differential scanning calorimetry (DSC). The DSC experiment allows ΔH for a transition to be measured and, because the system is at equilibrium at a transition and hence $\Delta G=0$, then ΔS can be evaluated ($=\Delta H/T$).

Now, from the molecular field approach to the biaxial nematic phase carried out by Straley [12] and by Boccara *et al*. in which they looked at a shape biaxiality approach to the N_B phase [13], a direct transition from the isotropic to N_B phase was found at the so-called Landau point where the shape biaxiality was optimal (figure 1). At the Landau point, $\Delta S=0$ and the transition is second order; as λ increases or decreases away from the ideal value of $1/\sqrt{6}$, the N–I transition moves from being second order to become first weakly first order and then more strongly first order. Typical values for $\Delta S/R$ for a first order N–I transition are $\geqslant 0.4$.

*Corresponding author. Email: d.bruce@york.ac.uk
Present address: Department of Chemistry, University of York, Heslington, York YO10 5DD.

Liquid Crystals
ISSN 0267-8292 print/ISSN 1366-5855 online © 2005 Taylor & Francis
http://www.tandf.co.uk/journals
DOI: 10.1080/02678290500160753

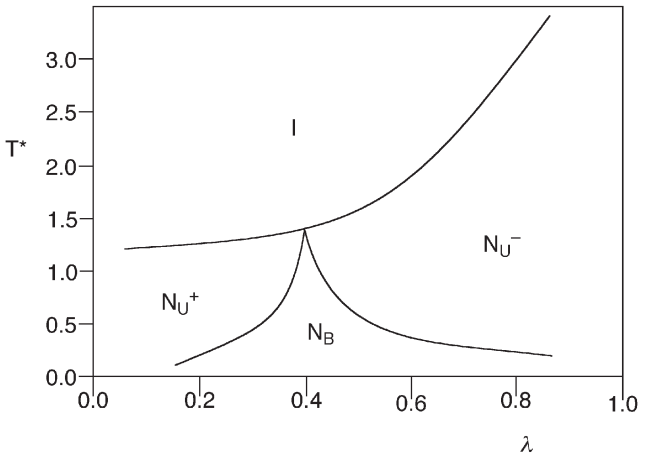

Figure 1. Dependence of clearing temperature on molecular biaxiality (λ) from a molecular mean field approach.

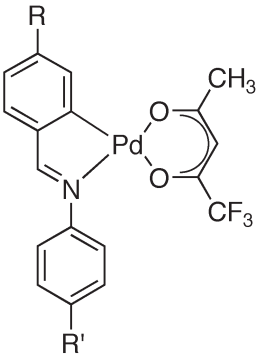

Figure 2. Palladium(II) complexes studied previously.

As discussed in [7, 8], theory and simulation can suggest directions for experiment and recently we reported on the design and synthesis of some *ortho*-metallated palladium(II) complexes (figure 2) which

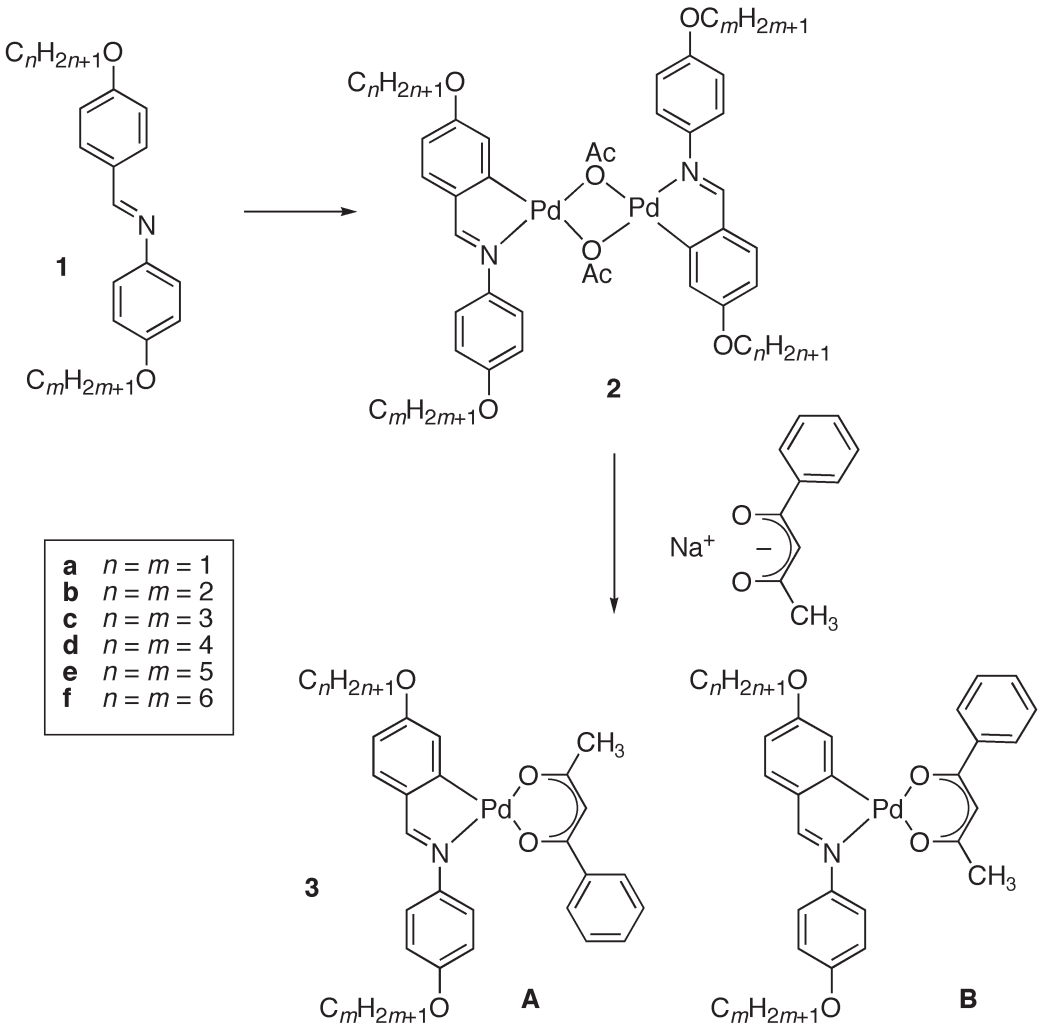

Figure 3. Synthesis of the target complexes.

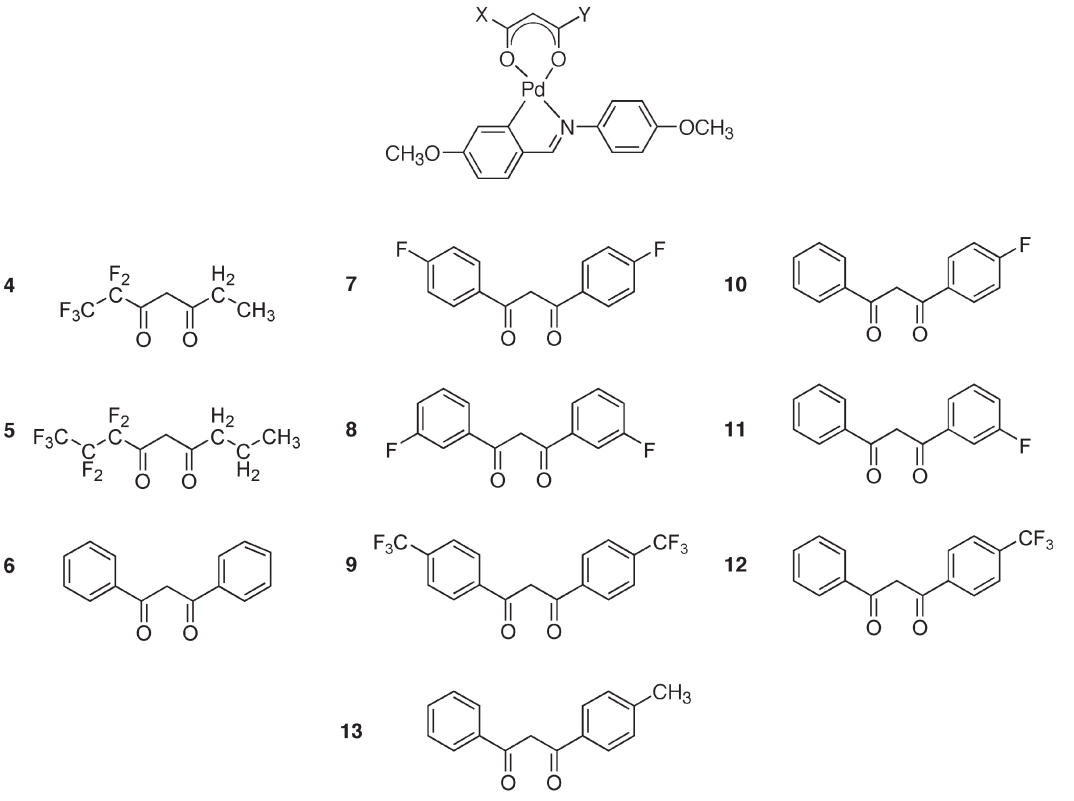

Figure 4. Structures of the β-diketonates used in this study. Compound numbers refer to resulting complexes.

Table 1. Crystallographic data for **3a**, **3f** and **4**.

Parameter	**3a**	**3f**	**4**
Empirical formula	$C_{25}H_{23}NO_4Pd$	$C_{35}H_{43}NO_4Pd$	$C_{22}H_{20}F_5NO_4$ Pd
Formula weight/g mol^{-1}	507.84	648.10	563.79
Temperature/K	150(2)	120(2)	120(2)
Crystal system	Orthorhombic	Monoclinic	Monoclinic
Space group	$P2_12_12_1$	$P2_1/n$	$P2_1/n$
Unit cell dimensions/Å	a=7.6079(15)	a=16.9350(2)	a=14.4378(17)
	b=11.184(2)	b=10.71940(10)	b=11.7300(13)
	c=24.611(5)	c=17.8635(3)	c=26.278(4)
		β=104.1420(10)	β=101.553(4)
Volume/Å^3	2094.0(7)	3144.53(7)	4360.1(10)
Z	4	4	8
Density (calculated) Mg m^{-3}	1.611	1.369	1.718
Absorption coefficient/mm^{-1}	0.919	0.628	0.923
Crystal	Prism; yellow	Block; orange	Blade; orange
Crystal size/mm^3	0.36 × 0.28 × 0.26	0.45 × 0.40 × 0.32	0.35 × 0.1 × 0.03
θ range for data collection	2.00–27.48°	2.97–27.49°	4.99–27.42°
Reflections collected	14032	35103	33450
Independent reflections	4673 [R_{int}=0.0344]	7179 [R_{int}=0.0563]	9744 [R_{int}=0.1359]
Completeness to θ=27.42°	98.8%	99.7%	98%
Goodness-of-fit on F^2	1.064	1.051	1.053
Final R indices [$F^2>2\sigma(F^2)$]	$R1$=0.0247, $wR2$=0.0554	$R1$=0.0323, $wR2$=0.0745	$R1$=0.1073, $wR2$=0.2669
R indices (all data)	$R1$=0.0295, $wR2$=0.0568	$R1$=0.0385, $wR2$=0.0776	$R1$=0.1609, $wR2$=0.3013
Largest diff. peak and hole	0.564 and −0.593 e Å^{-3}	1.172 and −0.920 e Å^{-3}	2.090 and −2.404 e Å^{-3}

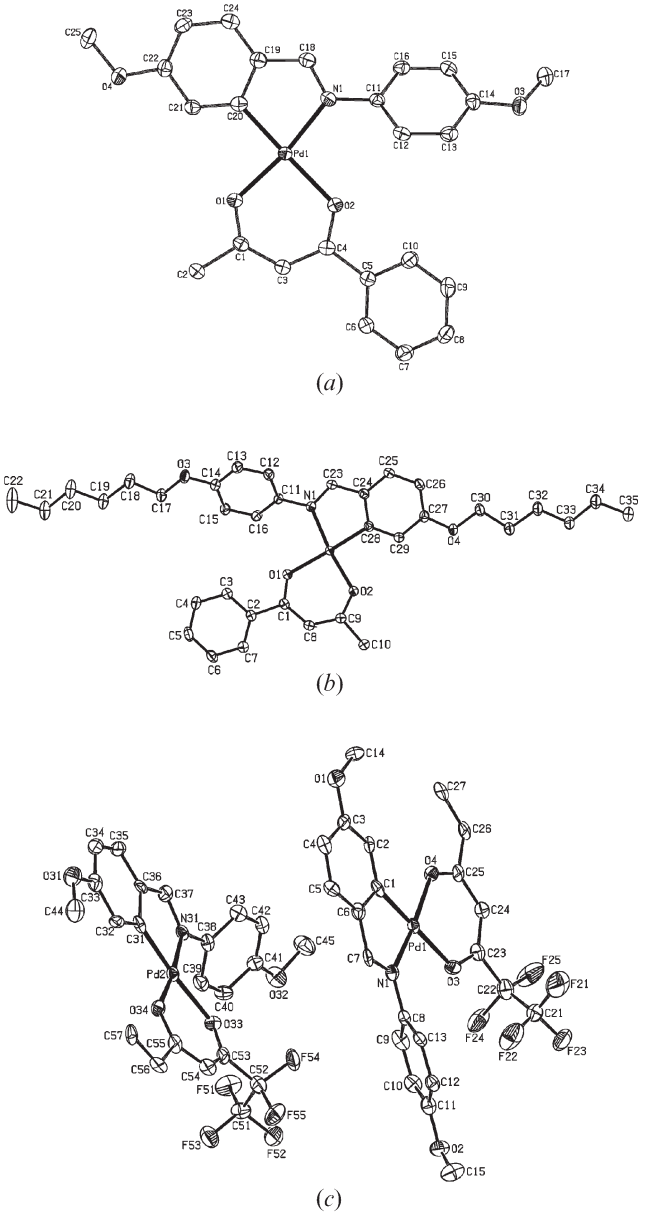

Figure 5. The molecular structures of compounds **3a**, **3f** and **4**.

showed small entropies of transition at the N–I transition, and similarly small transitional order parameters, S [14]. The complexes were designed on the basis that fluorocarbon groups prefer to self-associate as do hydrocarbon groups, and so it was reasoned that such preferential self-association might lead to the lateral correlations necessary to stabilize a N_B phase. In parallel with this work, a computational approach was adopted by Berardi and Zannoni in which they increased the attractive edge-to-edge potential in a modified Gay–Berne system and were able to show that this induced a N_B phase. Thus there was also a computational basis for the investigations undertaken [15].

This *ortho*-metallated palladium(II) scaffold is very attractive for the design of mesogenic species and has been exploited extensively by, in particular, the groups of Ghedini and Espinet [16]. Most relevant here is the fact that the synthetic protocol used (e.g. transformation of **2** to **3** in figure 3) allows the incorporation of a wide range of anionic ligands, which leads to considerable design flexibility. In this paper, we report the synthesis and characterization of a new series of such complexes as candidate biaxial materials, where it appears that the structural motif leads to the possibility of tuning the overall molecular shape through a calamitic–discotic 'transition'.

2. Results and discussion

2.1. *Synthesis*

The synthetic scheme is found in figure 3. The imine ligands **1** were readily prepared by the condensation of an alkoxybenzaldehyde with an alkoxyaniline under acid catalysis. Products were obtained as colourless solids in yields typically between 60 and 80% following crystallization; ^{1}H NMR spectroscopy showed the appearance of the imine hydrogen as a singlet at δ

Table 2. Selected bond lengths (Å), bond angles (°) and torsion angles (°).

	3a	**3f**	**4** (Molecule **A**)	**4** (Molecule **B**)
Pd–O	2.004(1)	2.088(1)	2.080(7)	2.070(7)
Pd–O	2.095(1)	2.011(1)	2.021(7)	2.014(7)
Pd–N	2.045(1)	2.045(1)	2.034(9)	2.040(8)
Pd–C	1.966(2)	1.978(2)	1.944(11)	1.954(11)
O–Pd–O	90.97(6)	91.03(6)	91.6(3)	91.8(3)
N–Pd–C	81.10(8)	81.27(7)	82.4(4)	82.2(4)
Pd–O–C–C	2.81(3)	5.42(2)	4.54(14)	7.70(15)
Pd–O–C–C	2.41(3)	0.0(3)	1.88(14)	0.43(14)
Pd–N–C–C	3.30(3)	1.45(2)	3.01(12)	3.81(11)
Pd–C–C–C	2.55(3)	5.63(2)	3.21(11)	1.34(11)

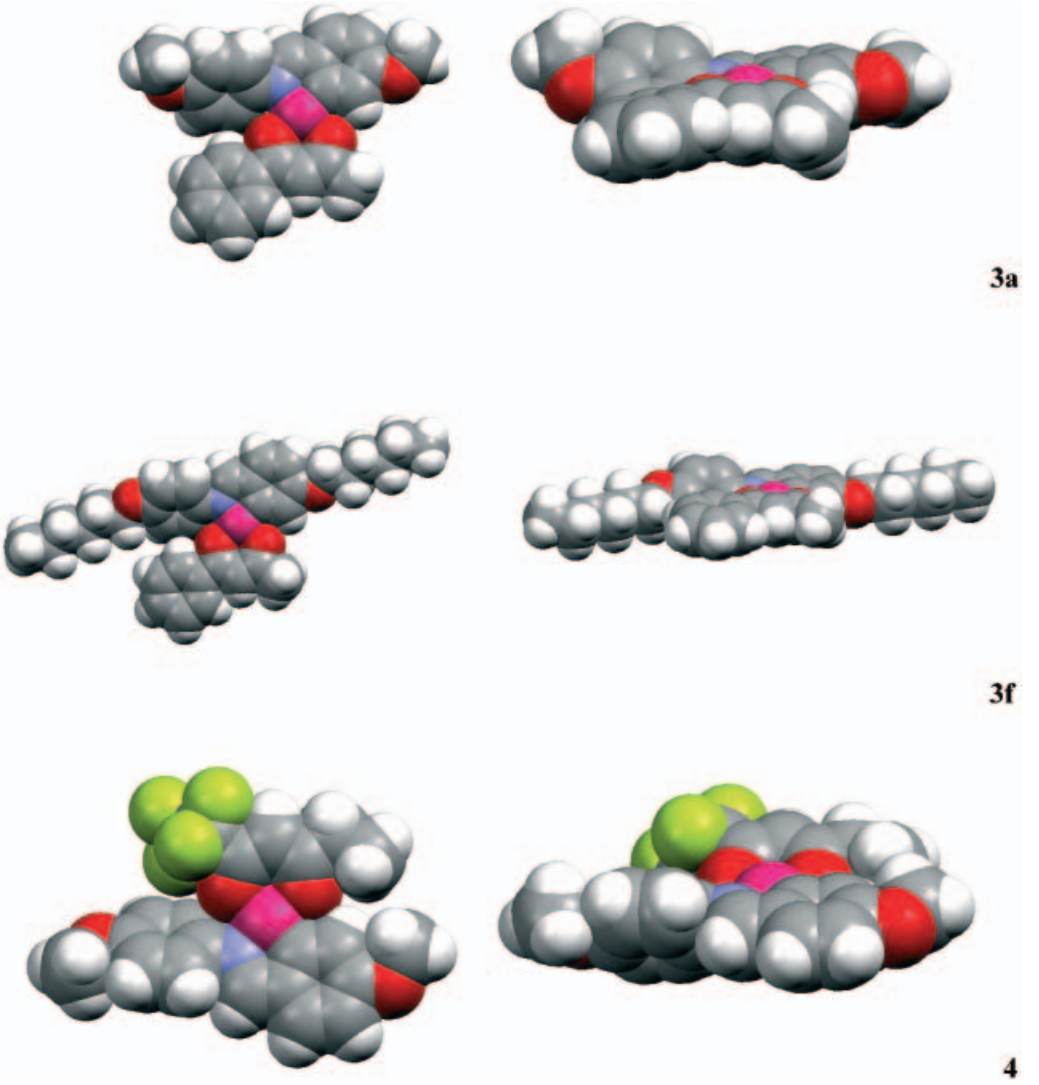

Figure 6. Space-filling representations of compounds **3a**, **3f** and **4** viewed (*a*) perpendicular and (*b*) parallel to the palladium square plane.

8.42. Reaction of the ligands with palladium acetate afforded the dinuclear di-μ-acetato complexes **2** in yields of around 90%. The target materials **3** were then obtained on cleaving the acetato bridge with the sodium salt of 1-phenylbutane-2,4-dione in CH_2Cl_2. Yields of the yellow product **3** were rather low and mostly in the range 30 to 40%. Clearly, **3** can exist as one of two isomers (**A** and **B**) in which the diketonate phenyl group is *syn* or *anti* with respect to the Pd–N bond. Nuclear Overhauser enhancement (nOe) NMR spectroscopy was used to identify the two isomers and it was found that the *anti*-isomer predominated, existing in a constant 2:1 ratio with the *syn*-isomer in solution. This ratio was reproducible with varying chain length and over several preparations, and so we were content that we were always dealing with the same material.

The synthesis was also undertaken of a series of complexes using imine **1a** where the diketonato ligand was varied as shown in figure 4 to give complexes **4** to **13**. These complexes were targeted to provide an understanding of how the structure of the diketonato co-ligand would influence the mesomorphism of this disc-like core. The β-diketonates associated with complexes **4** and **5** had been reported previously [17]; that associated with **6** was available commercially, while those associated with complexes **7** to **13** were synthesized by literature methods using a base-catalysed condensation between the appropriate methyl ester and methyl ketone [18–20].

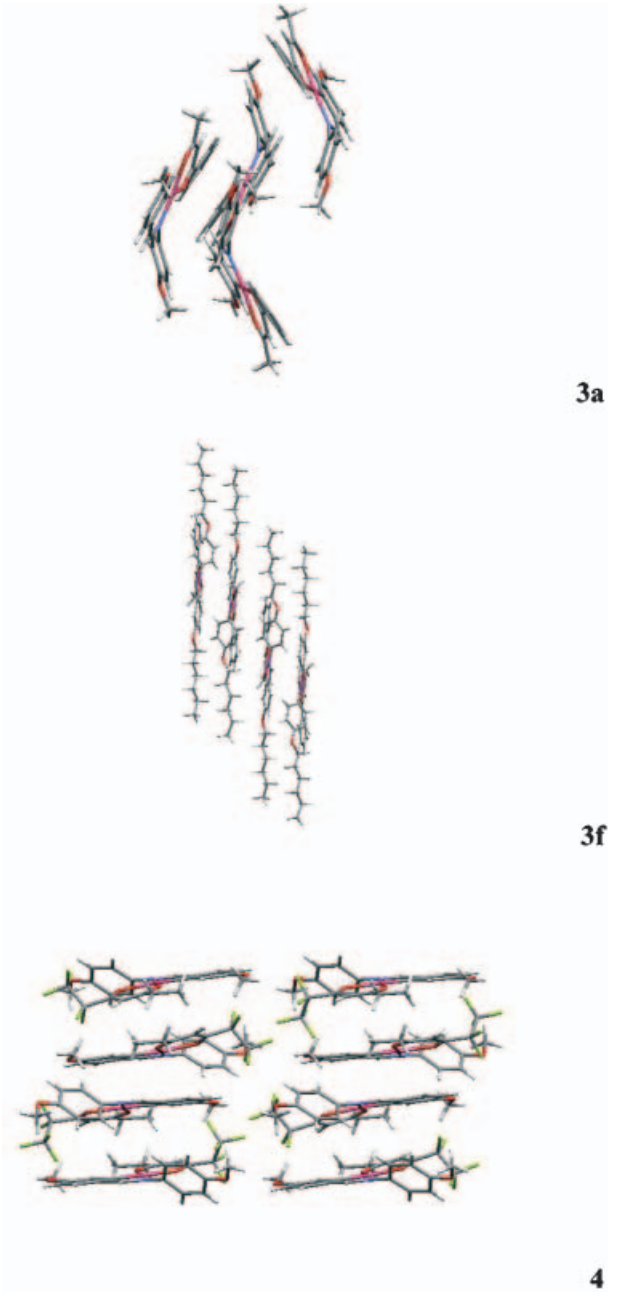

Figure 7. Crystal structure-packing motifs for compounds **3a**, **3f** and **4**.

2.2. *Crystal and molecular structure of 3a, 3f and 4*

In the case of complexes **3a**, **3f** and **4**, it was possible to obtain single crystals by crystallization from $CHCl_3$/MeOH (**3a**), acetone/hexane (**3f**) and dichloromethane/ethanol (**4**); crystallographic data are collected in table 1. Data were collected by means of combined ϕ and ω scans on a Nonius KappaCCD area detector situated at the window of a Nonius FR591 rotating anode (λMo-K_α=0.71073 Å). The structures were solved by direct methods, SHELXS-97 and refined using SHELXL-97 [21]. Hydrogen atoms were included in the refinement, but thermal parameters and geometry were constrained to ride on the atom to which they are bonded. The data were corrected for absorption effects using SORTAV [22]. Supplementary data in the form of CIF files have been deposited with the Cambridge Crystallographic Data Centre (Deposition numbers: CCDC217953, CCDC257544, CCDC257545 for **3a**, **3f** and **4**, respectively).

The structures of **3a**, **3f** and both molecules present in **4**, along with their atomic numbering schemes, are depicted in figures 5(*a–c*), respectively, whilst selected bond lengths, angles and torsions are given in table 2. From these figures it can be seen that all three structures are arranged in the less common *syn*-configuration. The ^{1}H NMR spectrum of a single crystal of **3a** shows only one isomer present, indicating that this is not due to isomerization in the solution phase and that this isomer is less soluble and crystallizes preferentially. In **3a** the chelate rings about the palladium centre are essentially planar with a maximum deviation from the mean plane of 0.078 Å, and the rings C5>C10, C11>C16 and C19>C24 are inclined to this plane at angles of 15.04°, 42.05° and 8.04°, respectively. The corresponding chelate rings about the palladium centre in **3f** are also planar with a maximum deviation from the mean plane of 0.084 Å, and the rings C2>C7, C11>C16 and C24>C29 are inclined to this plane at angles of 7.03°, 40.06° and 4.34°. In **4** the chelate rings about the palladium centre are essentially planar with a maximum deviation from the mean plane of 0.081 and 0.158 Å for Pd1 and Pd2, respectively, with the rings C1>C6 and C8>C13 (Pd1), and C31>C36 and C38>C43 for (Pd2) inclined to this plane at angles of 1.84°, 48.29°, 1.10° and 45.50°. Despite possessing one less ring the equivalent dihedral angles in **4** show remarkable agreement with those in **3a** and **3f**, indicating that all three compounds adopt very similar molecular conformations in terms of the disposition of the ligand ring systems about the palladium metal centre. This is supported by the strong agreement between the bond length, angle and torsional geometries shown in table 2.

Figure 6 shows space-filling representations (*a*) perpendicular and (*b*) parallel to the palladium square plane and indicates the molecular morphology to be that of a disc for structures **3a** and **4**. Conversely the view for **3f** indicates that the molecular morphology is a rod-like, elongated complex, although clearly the

Table 3. Thermal data for the new complexes.

Compound	Transition	T/°C	ΔH/kJ mol^{-1}	$\Delta S/R$
3a	Cr–I	165.0	37.7	10
	(I–N)	(94)	(0.04)	(0.01)
3b	Cr–I	182.7	45.6	12.0
	(I–N)	(108.5)	(0.4)	(0.1)
3c	Cr–I	153.7	18.7	5
	(I–N)	(94.7)	(0.2)	(0.04)
3d	Cr–I	131.9	34.2	10
	(I–N)	(113.6)	(0.4)	(0.07)
3e	g–I	152	—	—
	(I–N)	(99.6)	(0.1)	(0.04)
3f	Cr–SmA	89.8	35.6	12
	SmA–N	104.7	1.4	0.5
	N–I	127.6	0.3	0.1
4	Cr–I	107	27.6	9
5	Cr–I	98	37.0	12
6	Cr–I	149	60.5	18
7	Cr–I	222	40.7	10
	(SmA–I)	(199)	(3.1)	1
8	Cr–I	208	48.2	12
	(I–SmA)[a]	(173)		
9	Cr–I	249	49.5	12
10	Cr–I	205	37.1	9
	(SmA–I)	(139)	(1.8)	(0.5)
11	Cr–Cr′	188	40.8	11
	Cr′–I	203	14.0	4
	(I–SmA)[a]	(114)		
12	Cr–I	203	35.3	9
	(SmA–I)	(173)	(3.1)	(1)
13	Cr–I	210	41.5	10

[a]Transition occurs just before recrystallization; thermal data could not be obtained by DSC.

ligated β-diketonato group reduces the anisotropy considerably.

Figure 7 illustrates the packing motifs for each of the compounds **3a** (down the *c*-axis), **3f** (down the *b*-axis) and **4** (down the *a*-axis). It can be seen that a corrugated sheet motif is adopted for **3a**, whilst **3f** stacks as planar sheets and **4** adopts a layer type structure.

2.3. *Mesomorphism*

The mesomorphism of all the compounds was studied by polarizing optical microscopy and transitional enthalpies were recorded using a differential scanning calorimeter. The mesomorphism of the imines has been described previously and our data were consistent with that found in the LiqCryst database [23]; none of the dinuclear complexes, **2**, was mesomorphic. Results for the new compounds, **3a**–**f** to **13**, are collected in table 3.

All of the complexes **3** showed a nematic phase and in all but complex **3f**, the phase was monotropic; complex **3f** showed a SmA phase in addition. The variations in the optical textures of these complexes were of particular interest. Thus, while the shortest chain homologue, **3a**, showed a completely homeotropic texture, compounds **3b**, **3c** and **3d** exhibited textures where large homeotropic regions co-existed with a birefringent, marbled texture, typical of nematic phases. A further increase in the chain length led to compound **3e** which showed a similar mixed texture but with birefringent areas containing schlieren disclinations. Finally, complex **3f** exhibited textures of nematic and smectic phases typical for mesophases formed by rod-like molecules. It is also interesting to note (figure 8) that both the clearing point and clearing entropy of the complexes show a pronounced odd-even effect [24].

However, what is of particular significance in considering these materials is their shape and the magnitude of the clearing entropies. Figure 6 (*a*) shows the inherently disc-like nature of complex **3a** which suggests that the nematic phase ought to be N^- in nature. (Use of the more common notation, N_D, is avoided as a phase should be classified by its symmetry and the uniaxial nematic phase of any object has $D_{\infty h}$ symmetry.) Certainly the small magnitude of the clearing entropy is consistent with an N^- phase where clearing enthalpies/entropies do tend to be very much

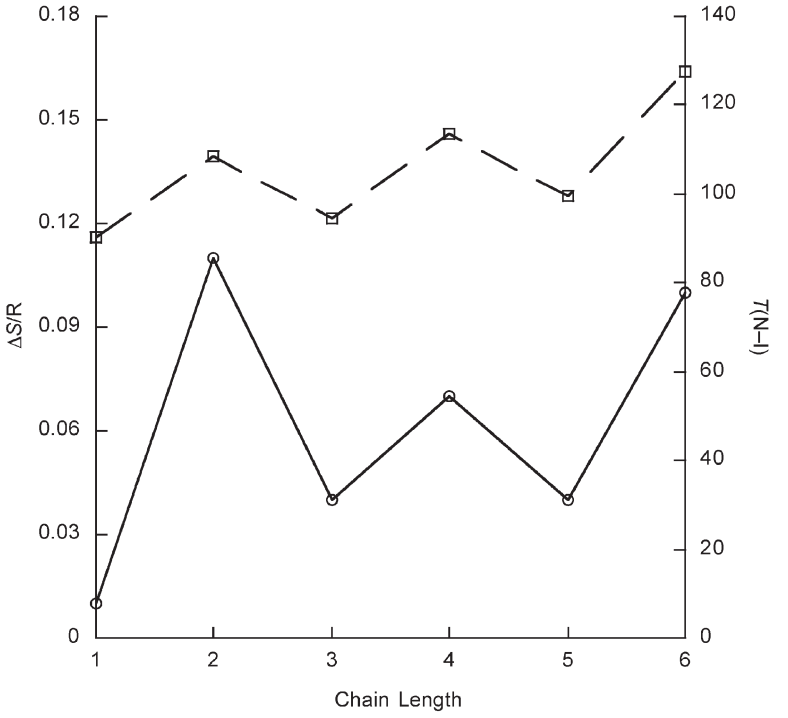

Figure 8. Variation in clearing temperature and clearing entropy as a function of chain length; ○ denotes $\Delta S/R$ and □ T_{NI}.

smaller that those found for calamitic materials where normally $\Delta S/R \geqslant 0.4$. Further, the optical texture found for **3a** was always homeotropic, which is another common feature of the N_D phase. It is also interesting to compare the nature of **3a**, which has no chains (if OMe is treated as simple functional group), with polychlorinated indenes and pseudoazulenes described by Ros *et al*. [25] that showed a columnar phase despite having only a very small core and no peripheral chains (figure 9). This supports the assertion that it is likely that the nematic phase of **3a** can be classified as N^-.

What makes this observation particularly interesting is that when the chain length is increased to six (**3f**), the complex shows both a N and SmA phase—the latter a characteristic of a calamitic material, which implies that if **3a** is a disc then in varying the chain length from one to six, the complex has gone through a rod–disc transition. This is precisely the behaviour indicated in figure 1, where at one extreme λ defines a rod ($\lambda=0$) and at the other, a disc ($\lambda=\sqrt{3}/2$). It is also noticeable that $\Delta S/R$ for **3f**$=0.1$ which is significantly smaller than that expected for an N–I transition in a calamitic material. It may then be significant, as explained above, that as the value of λ moves away from the Landau point value of $1/\sqrt{6}$, the N–I transition becomes weakly, and then more strongly, first order.

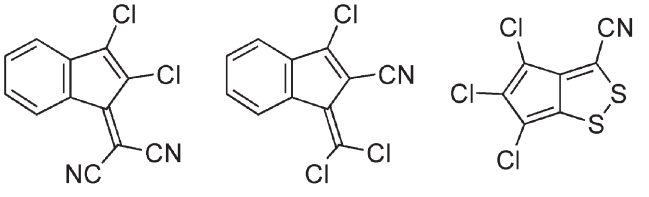

Figure 9. Examples of small, disc-like molecules showing columnar phases.

Taken together, these observations suggest that somewhere in the range $1 \leqslant n,m \leqslant 6$, these palladium(II) complexes undergo a rod–disc transition and, if that point could be pinpointed, then it may be possible to identify a N_B phase. Of course, because the ligands are unsymmetric, then for these values of n and m, there are some thirty-six complexes and so finding the right one, if indeed it exists, will be a challenge—and one we hope to pursue with Geoffrey Luckhurst well into his formal retirement!

Next, complexes **4** to **13** are considered in which the terminal chains on the imine are both methoxy, and the nature of the β-diketonate was varied. The β-diketonate in **4** and **5** contains extended alkyl and perfluoroalkyl chains to see if an increase in the fluorocarbon area would further facilitate achieving our target. In fact, the results were disappointing and while the melting points were reduced to around 100°C, it is suspected that the bulky nature of the perfluoro-ethyl and -propyl groups has destabilized *both* the crystal and the liquid crystal

phases—the latter to a much greater extent as no monotropic phases were observed. Complex **6**, a more symmetric version of **3a**, was also non-mesomorphic with a melting point that, curiously, was a little lower—something not necessarily expected given that **6** is a pure compound (recall **3a** is a mixture) as well as being symmetric. An attempt to lower the symmetry by introducing a methyl group into the diketonate (complex **13**) was similarly unproductive and resulted in an even higher melting point.

Having found that the use of extra perfluorocarbon did not lead to the desired properties, attention then turned to the introduction of lateral dipoles via the use of different fluorophenyl isomers as found in complexes **7**, **8**, **10** and **11**, as well as by employing a trifluoromethyl group in **9** and **12**. Of these six new complexes, **9** was non-mesomorphic but the remaining complexes were mesomorphic, in each case showing a monotropic SmA phase. Complex **9**, containing two trifluoromethylphenyl groups, melted at almost 250°C with no monotropic phase seen on cooling, while the unsymmetric analogue, **12**, showed a lower melting point and a monotropic SmA phase some 30°C below the melting point. Of the two difluoro complexes, **7** and **8**, the former, with the fluorines in the 4-position on the phenyl ring, melted at the higher temperature (222°C) and showed a monotropic SmA phase at 199°C, while the latter melted at 208°C with the SmA phase seen at 173°C. Reducing the symmetry of **7** to give **10** lowered the melting point slightly to 205°C, significantly destabilizing the SmA phase, which now appeared at 139°C. Lowering the symmetry of **8** to give **11** again had little effect on the melting point, but now the SmA phase was very strongly monotropic and was observed very briefly ahead of crystallization.

What is striking about these results is that the introduction of one or two $C_{aromatic}$–F dipoles was sufficient to promote a layering of the complexes, despite the fact that the imine chains were both methoxy. This remarkable result shows how finely balanced this palladium system really is, as such a small change leads to a significant change in the observed mesophase. However, not only is the result remarkable, but it is also very encouraging as it shows that the lateral correlations present in the system can be tuned—precisely what was required and precisely the route identified to try to realize this elusive phase. The search continues…

3. Experimental

Dichloromethane was distilled from calcium hydride; other chemicals were used as supplied. Proton and carbon NMR spectra were recorded on a Bruker DFX 400 MHz or ACF-300 spectrometer. Elemental analysis was performed in the Department of Chemistry, University of Exeter. Analysis by DSC was carried out using a Perkin-Elmer DSC7 instrument using various heating rates. Mesomorphism was studied by hot stage polarizing microscopy using a Zeiss Labpol microscope equipped with a Linkam TH600 hot stage and PR600 temperature controller. Mesophases were assigned by their optical textures.

Suitable single crystals were selected and data collected on a Bruker Nonius KappaCCD Area Detector at the window of a Bruker Nonius FR591 rotating anode ($\lambda_{Mo\text{-}K\alpha}$=0.71073 Å) driven by COLLECT [26] and DENZO [27] software at 120 K. Structures were determined in SHELXS-97 [28] and refined using SHELXL-97 [29].

3.1. *Synthesis of ligands*

Imines (**1**) were prepared by condensation of the relevant benzaldehyde and aniline in ethanol, catalysed by acetic acid. CHN and NMR data were good and transition temperatures agreed with literature values [23].

The β-diketonate ligands for complexes **4** and **5** were prepared according to literature procedures [17] or by analogy therewith (**7** to **13** [18–20] were crystallized from ethanol); ligands for **3** and **6** were purchased from Aldrich or Lancaster. *1,3-Bis(3′-fluorophenyl)-1,3-propanedione*: colourless crystals, m.p. 127°C; *1,3-bis(4′-trifluoromethylphenyl)-1,3-propanedione*: pink crystals, m.p. 130°C; *1-(4′-trifluoromethylphenyl)-3-phenyl-1,3-propanedione*: colourless crystals, m.p. 101°C.

3.2. *Preparation of sodium salts of* β*-diketonate derivatives*

The sodium salts of β-diketonate derivatives were prepared by reacting the corresponding β-diketone with sodium ethoxide (1:1 molar ratio) in refluxing petroleum ether for 4 h. A white or off-white precipitate developed for all β-diketonate derivatives except **4** and **5**; it was filtered off and washed with petroleum ether. For **4** and **5** the solvent was removed *in vacuo* to give a white solid. The sodium salts were used in the next step without further purification. Their purity, checked by NMR (in DMSO-d_6), was >90%.

3.3. *Synthesis of the* μ*-acetato complexes, 2*

The synthesis of **2f** is described as typical. To a solution of palladium acetate (2.03 g, 3 mmol) in dichloromethane (25 cm^3) was added Schiff's base **1f** (3.42 g, 9 mmol) and the mixture was stirred and heated under reflux for 18 h. After cooling and evaporation of the solvent, the yellow–green precipitate was washed with cold acetone and air dried (4.44 g, yield=91%).

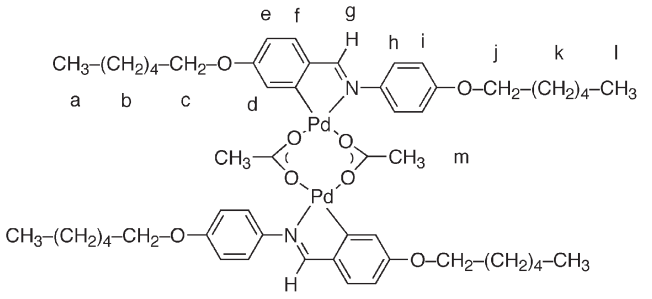

^{1}H NMR (δ, 400 MHz, $CDCl_3$): 7.45 (1H, **g**, s), 7.11 (1H, **f**, d, $^3J_{HH}$=8.3 Hz), 6.66 (4H, **h**+**i**, m), 6.55 (1H, **e**, dd, $^3J_{HH}$=8.3 Hz, $^4J'_{HH}$=2.4 Hz), 6.06 (1H, **d**, d, $^4J_{HH}$=2.4 Hz), 3.94–3.55 (4H, **c**+**j**, m), 1.83 (3H, **m**, s), 1.76–1.38 (16H, **b**+**k**, m), 0.92 (6H, **a**+**l**, t, J_{HH}=6.9 Hz).

All others dinuclear complexes **2** were synthesized following the same procedure. Their ^{1}H NMR spectra are identical except for corresponding decrease in integration of the hydrogens **b** and **k** of the alkoxy chains at $\delta \approx 1.76$–1.38. Yields and analytical data for these compounds are collected in table 4.

3.4. *Synthesis of mononuclear complexes, 3*

The synthesis of **3f** is described as typical. Solid sodium 1-phenyl-3-methylacetylacetonate (151 mg, 0.82 mmol) was added to a solution of [LPd(μ-OAc)]$_2$**2f** (435 mg, 0.41 mmol) in dichloromethane (40 cm^3) and the mixture stirred at room temperature for 24 h. Evaporation of the solvent gave a yellow powder, which was purified by chromatography on silica with a mixture of diethyl ether/petroleum ether (1/1) as eluant to give a yellow solid (154 mg, yield=29%). Two isomers are distinguishable in the ^{1}H NMR spectrum for protons **m**, **p** and **q** in a ratio 2:1 (**A**/**B** respectively). NMR labelling scheme:

Isomer A:

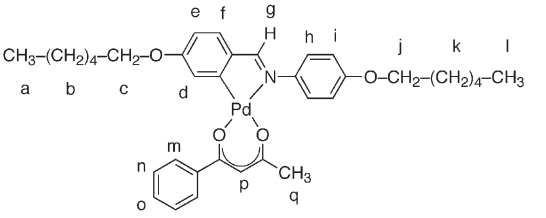

Isomer B:

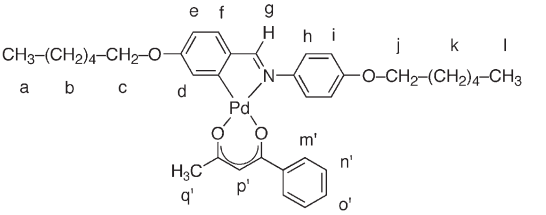

^{1}H NMR (δ, 300 MHz, $CDCl_3$): 8.02 (1H, **g**, s), 7.97 (2H, **m**′, m), 7.72 (2H, **m**, m), 7.48–7.30 (6H, **n**+**n**′+**o**+**o**′+**h**+**f**, m), 7.17 (1H, **d**, d, $^4J_{HH}$=2.5 Hz), 6.95 (2H, **i**, d, AA′XX′, J=8.3 Hz), 6.65 (1H, **e**, m), 6.09 (1H, **p**, s), 6.02 (1H, **p**′, s), 4.14–3.99 (4H, **c**+**j**, m), 2.26 (3H, **q**, s), 2.06 (3H, **q**, s), 1.88–1.26 (16H, **b**+**k**, m), 0.94 (3H, **a**+**l**, m).

Table 4. Yields and microanalytical data for the complexes.

Compound	Yield / %	% C found (calc.)	% H found (calc.)	% N found (calc.)
2a	93	49.9 (50.3)	3.9 (4.2)	3.1 (3.4)
2b	88	51.8 (52.6)	4.7 (4.9)	3.0 (3.2)
2c	91	55.0 (54.6)	5.3 (5.5)	2.7 (3.0)
2d	87	56.1 (56.4)	5.9 (6.0)	2.8 (2.9)
2e	88	58.1 (58.0)	6.4 (6.4)	2.4 (2.7)
2f	93	59.1 (59.4)	6.8 (6.8)	2.4 (2.5)
3a	45	58.8 (59.1)	4.5 (4.6)	2.5 (2.8)
3b	37	60.7 (60.5)	5.1 (5.1)	2.4 (2.6)
3c	14	61.3 (61.8)	5.4 (5.5)	2.5 (2.3)
3d	30	62.3 (62.9)	5.9 (6.0)	2.2 (2.4)
3e	37	63.5 (63.9)	6.5 (6.3)	2.2 (2.3)
3f	29	64.5 (64.9)	6.7 (6.7)	2.0 (2.2)
4	87	46.7 (46.9)	3.4 (3.6)	2.5 (2.5)
5	85	53.0 (53.2)	5.4 (5.5)	1.9 (1.8)
6	90	63.0 (63.2)	4.4 (4.4)	2.4 (2.5)
7	58	64.4 (64.4)	6.0 (5.8)	1.7 (1.9)
8	29	59.0 (59.4)	3.5 (4.0)	1.9 (2.3)
9	23	54.0 (54.4)	3.3 (3.4)	1.7 (2.0)
10	47	61.0 (61.2)	3.9 (4.3)	2.1 (2.4)
11	65	61.2 (61.3)	4.1 (4.1)	2.2 (2.4)
12	47	57.9 (58.4)	3.7 (3.8)	2.1 (2.2)
13	37	63.5 (63.8)	4.6 (4.7)	2.3 (2.0)

Yields and analytical data for these compounds are collected in table 4.

3.5. *Synthesis of complexes 4 to 13*

Complex **2a** (0.1 mmol) was dissolved in dichloromethane (25 cm^3). The sodium salt of the β-diketonate derivative (0.25 mmol) was added and the mixture stirred at room temperature for 18 h. The solvent was evaporated and the residue purified on silica using dichloromethane as eluant. Crystallization from dichloromethane/ethanol gave the mononuclear complexes as yellow crystals. Analytical data are found in table 4.

Acknowledgements

We thank the EU, NEDO (LO) and NATO (VC) for support. It is also a great pleasure to acknowledge our long collaboration with Geoffrey Luckhurst on the subject of the biaxial nematic phase. Geoffrey's enthusiasm for science is absolutely contagious and our collaboration has been a real joy—long may it continue!

References

[1] L.J. Yu, A. Saupe. *Phys. Rev. Lett.*, **45**, 1000 (1980).
[2] A.A. de Melo Filho, A. Laverde, Jr, F.Y. Fujiwara. *Langmuir*, **19**, 1127 (2003).
[3] F. Hessel, H. Finkelmann. *Polym. Bull.*, **15**, 349 (1986).
[4] K. Severing, K. Saalwächter. *Phys. Rev. Lett.*, **92**, 125501 (2004).
[5] L.A. Madsen, T.J. Dingemans, M. Nakata, E.T. Samulski. *Phys. Rev. Lett.*, **92**, 145505 (2004).
[6] B.R. Acharya, A. Primak, S. Kumar. *Phys. Rev. Lett.*, **92**, 145506 (2004).
[7] D.W. Bruce. *Chem. Recv.*, **4**, 10 (2004).
[8] G.R. Luckhurst. *Thin solid Films*, **393**, 40 (2001).
[9] K. Praefcke, D. Blunk, D. Singer, J.W. Goodby, K.J. Toyne, M. Hird, P. Styring, H. Norbert. *Mol. Cryst., liq. Cryst.*, **323**, 231 (1998).
[10] K. Praefcke, B. Kohne, B. Gündogan, D. Singer, D. Demus, S. Diele, G. Pelzl, U. Bakowsky. *Mol. Cryst., liq. Cryst.*, **198**, 393 (1991).
[11] Y. Galerne. *Mol. Cryst., liq. Cryst.*, **323**, 211 (1998).
[12] J.P. Straley. *Phys. Rev. A*, **10**, 1881 (1974).
[13] N. Boccara, R. Mejdani, L. de Seze. *J. de Phys.*, **38**, 149 (1977).
[14] L. Omnès, B.A. Timimi, T. Gelbrich, M.B. Hursthouse, G.R. Luckhurst, D.W. Bruce. *Chem. Commun.*, 2248 (2001).
[15] R. Berardi, C.J. Zannoni. *Chem. Phys.*, **113**, 5971 (2000).
[16] This work is well reviewed by B. Donnio, D. Guillon, R. Deschenaux, D.W. Bruce. In *Comprehensive Coordination Chemistry II: From Biology to Nanotechnology*, J.A. McCleverty, T.J. Meyer (Eds), Vol. 7, Chap. 7.9 Vol. Ed. M., Fujita, A.K., Powell, Elsevier, Oxford (2003).
[17] R.A. Moore, R. Levine. *J. org. Chem.*, 1439 (1964).
[18] J.-P. Anselme. *J. org. Chem.*, **32**, 3716 (1967).
[19] W. Adam, H.M. Harrer, W.M. Nan, K. Peters. *J. org. Chem.*, **59**, 3786 (1994).
[20] W. Franek. *Monatsh. Chem.*, **127**, 895 (1996).
[21] G.M. Sheldrick. *SHELX* suite of programs for crystal structure solution and refinement, University of Göttingen, Germany (1997).
[22] R.H. Blessing. *Acta Cryst.*, **A51**, 33 (1995).
[23] *LiqCryst Database*, LCI Publisher, Hamburg.
[24] D. Demus. In *Handbook of Liquid Crystals*, D. Demus, G.W. Gray, J. Goodby, H.-W. Spiess, V. Vill (Eds), Vol. 1, Chap. VI, Wiley-VCH, Chichester (1998).
[25] J. Barbera, O.A. Rakitin, M.B. Ros, T. Torroba. *Angew. Chem. int. Edn. Engl.*, **37**, 296 (1998).
[26] R. Hooft. Collect: Data collection software, Nonius B.V. (1998).
[27] Z. Otwinowski, W. Minor. *Methods in Enzymology*, Vol. 276, pp. 307–326, C.W. Carter, Jr, R.M. Sweet (Eds), Academic, New York (1997).
[28] G.M. Sheldrick. *Acta Cryst.*, **A46**, 467 (1990).
[29] G.M. Sheldrick. University of Göttingen, Germany (1997).